Electronic Structure and Thermoelectric Power Factor of Na_xCoO_2 from First-Principles Calculation *

Peng-Xian Lu(路朋献)[1**], Rui-Xia Zhao(赵瑞霞)[2]

[1] College of Materials Science and Engineering, Henan University of Technology, Zhengzhou 450001
[2] Department of Civil Engineering and Architecture, Henan Technical College of Construction, Zhengzhou 450001

(Received 4 November 2016)

To investigate the relationship between the electronic structure and the power factor of Na_xCoO_2 ($x = 0.3$, 0.5 and 1.0), the first-principles calculation is conducted by using density functional theory and the semi-classical Boltzmann theory. Our results suggest that with the decreasing Na content, a transition from semiconductor to semimetal is observed. $Na_{0.3}CoO_2$ possesses a higher electrical conductivity at 1000 K due to its increased density of states near the Fermi energy level. However, an optimal Seebeck coefficient at 1000 K is obtained in $Na_{0.5}CoO_2$ because of its broadened band gap near the Fermi energy level. Consequently, a maximum power factor is realized in $Na_{0.5}CoO_2$. Thus our work provides a complete understanding of the relationship between the electronic structure and the thermoelectric power factor of Na_xCoO_2.

PACS: 71.20.Nr, 72.20.Pa DOI: 10.1088/0256-307X/34/3/037101

Thermoelectric materials, which can be used as solid-state Peltier coolers or power generators from waste heat, will play an important role in solving the global fossil energy crisis and minimizing environmental pollution.[1] A material with an excellent thermoelectric performance needs a high electrical conductivity, a large Seebeck coefficient and a low thermal conductivity simultaneously.[2] Recently, sodium cobalt oxide Na_xCoO_2 has been regarded as an encouraging thermoelectric material due to its lower cost, nonpoisonous nature, simple synthesis procedure and the antioxidization in oxidized atmosphere for a long time.[3,4] Many efforts in improving the thermoelectric properties of Na_xCoO_2 were made on either improving the Seebeck coefficient, or increasing the electrical conductivity and decreasing the thermal conductivity.

The experimental results have indicated that Na_xCoO_2 possesses a large Seebeck coefficient, a small electrical conductivity and meanwhile a high thermal conductivity.[5] The power factor of Na_xCoO_2 could be enhanced largely by altering x.[6] Moreover, the dependence of thermal conductivity on Na fractions x in the middle range was relatively weak and introducing Co vacancies resulted in a significant lattice thermal conductivity reduction.[7] Doping has been viewed as an effective route to improve the thermoelectric properties of Na_xCoO_2. Sr- or Ag-doping at Na sites can cause an increasing Seebeck coefficient but a decreasing thermal conductivity, although the electrical conductivity can also decrease slightly.[8,9] The electrical conductivity of the $Na_xCo_{1-y}Pb_yO_2$ with Pb doped at Co sites was improved, meanwhile the thermal conductivity was suppressed and the Seebeck coefficient was changed slightly.[10] The thermoelectric properties of $Na_{0.8}Zn_xCo_{1-x}O_2/(ZnO)(y)$ were also investigated. Doping Zn ions led to simultaneous increase in electrical conductivity and enhancement in thermopower. Such an increase in electrical conductivity was ascribed to the improved mobility of carriers, while the enhancement of thermopower was originated from the geometric relaxation of distorted CoO_6 octahedra caused by partial Zn substitution.[11] Meanwhile, theoretical calculations were widely conducted to reveal the mechanism of the electron and phonon transport in Na_xCoO_2. The thermoelectric properties of Na_xCoO_2 vary with its stoichiometry, structural defects, temperature and nanosheet geometry.[7] Its thermal conductivity could be suppressed significantly by an Einstein-like rattling mode at low energy.[12] Moreover, doped atoms could lead to a metal-insulator transition at low temperature in $Na_{0.8}Co_{1-x}Sm_xO_2$.[13] The formation energies of defects and the resultant changes in electronic structure of Na_xCoO_2 were evaluated using first-principles calculation.[14] In addition, the thermoelectric properties of the Na_xCoO_2 were also investigated using a simple lattice dynamical model or the Boltzmann theory.[15,16]

To the best of our knowledge, there have been no reports demonstrating the relationship among the electronic structure and the thermoelectric properties of Na_xCoO_2. Therefore, our work aims at providing a complete understanding on the relationship between the electronic structure and the thermoelectric properties of Na_xCoO_2 using first-principles calculation.

Na_xCoO_2 with different x ($x = 0.3$, 0.5 and 1.0) has different crystal structures, and its lattice param-

*Supported by the Science Foundation of Henan University of Technology under Grant No 2015XTCX10.
**Corresponding author. Email: pengxian_lu@haut.edu.cn
© 2017 Chinese Physical Society and IOP Publishing Ltd

eter and the atoms site can be obtained through the inorganic crystal structure data (ICSD, findit 2008 software).[17–19] Calculation was performed using the Cambridge serial total energy package (CASTEP), a first-principle pseudopotential method based on the density-functional theory (DFT).[20] The used pseudopotential was the norm-conserving pseudopotential. As for the approximation of the exchange correlation term of the DFT, the generalized gradient approximation (GGA) of Perdew was adopted with the Perdew–Burke–Ernzerhof parameters. The cutoff energy of atomic wave functions was set at 830 eV. Sampling of the irreducible wedge of the Brillouin zone was performed with a regular Monkhorst-Pack grid of special k-points, which was $12 \times 12 \times 4$. All atomic positions in the models have been relaxed according to the total energy and force using the BFGS scheme, based on the cell optimization criterion (RMs force of 0.01 eV/nm, displacement of 0.00005 nm). The calculation of total energy and electronic structure was followed by cell optimization with SCF tolerance of 5.0×10^{-6} eV. The partial density of states (PDOS) for electrons was obtained by broadening the discrete energy levels using a smearing function of full width at half maximum (FWHM) (0.05 eV) on a grid of k-points generated by the Monkhorst–Pack scheme.[21]

The effective mass of carriers m^* is obtained by differentiating the energy at Fermi energy level twice with respect to the wave vector of the high symmetric points in the Brillouin zone,

$$m^* = \hbar^2 / \Big(\frac{\partial^2 E}{\partial k^2} \Big), \tag{1}$$

where h is the Plank reduced constant, E is the energy band near the Fermi energy level, and k is the wave vector of the high symmetric points in the Brillouin zone. As for a semiconductor characteristic ($Na_{1.0}CoO_2$ and $Na_{0.5}CoO_2$), the four energy bands near the Fermi level in the valence band top are selected to calculate the thermoelectric parameters. However, in total four energy bands involving two bands above the Fermi level in the conduction band bottom and two bands below the Fermi energy level in the valence band top are selected to calculate the thermoelectric parameters for the semimetal behavior ($Na_{0.3}CoO_2$). The Fermi energy E_F^0 is the highest energy level occupied by electrons at 0 K,

$$E_F^0 = \frac{\hbar^2 k_0^2}{2m^*} = \frac{k_0^2}{2} \frac{\partial^2 E}{\partial k^2}, \tag{2}$$

where k_0 is the radius of the spherical surface with an energy $E = E_F^0$ at k space, m^* is the effective mass of carriers, E is the energy band, and k is the wave vector in the Brillouin zone. The temperature dependence of the Fermi energy is calculated by

$$E_F = E_F^0 \Big[1 - \frac{\pi^2}{12} \Big(\frac{k_B T}{E_F^0} \Big)^2 \Big], \tag{3}$$

where E_F^0 is the Fermi energy at 0 K, T is the absolute temperature, and k_B is the Boltzmann constant. The Fermi–Dirac distribution function $(-\frac{\partial f}{\partial E})$ is written as

$$\Big(-\frac{\partial f}{\partial E} \Big) = \frac{1}{k_B T} \frac{1}{(e^{(E-E_F)/k_B T} + 1)} \cdot \frac{1}{(e^{-(E-E_F)/k_B T} + 1)}, \tag{4}$$

where E is the energy band, E_F is the Fermi energy, and T is the absolute temperature. The group velocity of carriers $\upsilon_e(E)$ is calculated by differentiating the energy with respect to the wave vector in the Brillouin zone.[22] Consequently, the electrical conductivity and the Seebeck coefficient are defined as[23]

$$\sigma = \frac{e^2}{3} \int dE \Big(-\frac{\partial f}{\partial E} \Big) g(E) \tau(E) \upsilon^2(E), \tag{5}$$

$$\alpha = \frac{e}{3T\sigma} \int dE \Big(-\frac{\partial f}{\partial E} \Big) g(E) \tau(E) \upsilon^2(E)(E - E_F), \tag{6}$$

where e is the electron charge, $(-\frac{\partial f}{\partial E})$ is the Fermi distribution function, $g(E)$ is the density of states (DOS), $\upsilon_e(E)$ is the group velocity of electrons, E and E_F are the energy band and the Fermi energy, respectively, and $\tau(E)$ is the relaxation time, which can be simplified to an energy-independent constant equal to 6.5×10^{-25} s using the experimental electrical conductivity. Therefore, the power factor is determined by

$$P = \alpha^2 \sigma, \tag{7}$$

where α is the Seebeck coefficient, and σ is the electrical conductivity.

The band structures of Na_xCoO_2 (x = 0.3, 0.5, 1.0) are shown in Figs. 1(a)–1(c), respectively. It can be seen that $Na_{1.0}CoO_2$ and $Na_{0.5}CoO_2$ possess a typical semiconductor behavior with indirect energy gaps of about 0.40 eV and 1.04 eV near the Fermi energy level, respectively. However, $Na_{0.3}CoO_2$ exhibits a typical semimetal characteristic since several energy bands exist across the Fermi energy level. Moreover, in comparison with $Na_{1.0}CoO_2$, an obvious anisotropy of the band structure for $Na_{0.3}CoO_2$ and $Na_{0.5}CoO_2$ can be observed because the band curves along the H–K direction are very flat while very steep along the K–G direction. In addition, the much more extrema of the band structure existing in $Na_{0.3}CoO_2$ and $Na_{0.5}CoO_2$ will be beneficial to increase their electrical conductivities. It should also be noted that the effective masses of carriers in $Na_{0.3}CoO_2$ and $Na_{0.5}CoO_2$ (m^*/m_e equals 3.0 and 3.7, respectively) are larger than that in $Na_{1.0}CoO_2$ (m^*/m_e equals 1.8) since the width of the band structures at the bottom of conduction band is widened, which is helpful for the enhancement of their Seebeck coefficients according to

$$E_{gap} = 2eT\alpha_{max}, \tag{8}$$

where $E_{\rm gap}$ is the band gap energy, e is the electron charge, T is the absolute temperature, and $\alpha_{\max}$ is the maximum Seebeck coefficient.[24]

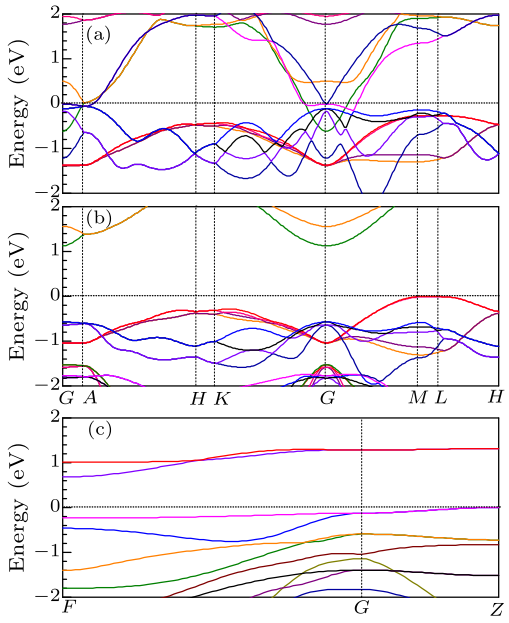

Fig. 1. Band structures of Na_xCoO_2: (a) $Na_{0.3}CoO_2$, (b) $Na_{0.5}CoO_2$ and (c) $Na_{1.0}CoO_2$.

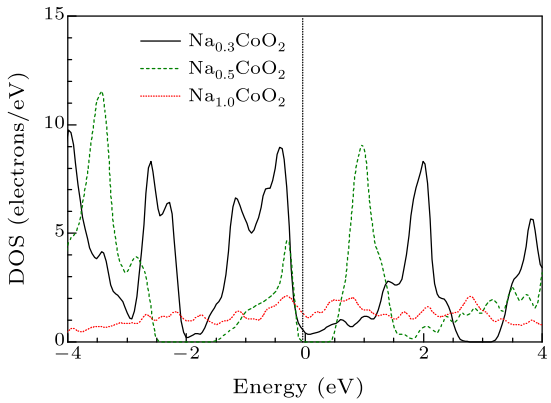

Fig. 2. DOS of Na_xCoO_2.

The density of states (DOS) of Na_xCoO_2 ($x = 0.3$, 0.5, 1.0) are presented in Fig. 2. In general, the electrical conductivity is mainly determined by the concentration of carriers near the Fermi energy level.[25] The low DOS of 2.15 electron/eV for $Na_{1.0}CoO_2$ may be a main reason for its small electrical conductivity. However, the increasing DOSs of 9.0 electron/eV and 4.0 electron/eV for $Na_{0.3}CoO_2$ and $Na_{0.5}CoO_2$ are beneficial to enhancing their electrical conductivity. The pseudogap energy, an energy gap between the nearest two peaks near Fermi energy level in the DOS curve, can reflect the covalent bonding strength between the parent atoms. The pseudogap energy of $Na_{1.0}CoO_2$ bulk is merely 1.00 eV, which indicates that the relatively weak covalent bonding would result in a low phonon vibration frequency and thus a small phonon thermal conductivity according to

$$\omega = \sqrt{\frac{k}{m}}, \tag{9}$$

where ω is the phonon vibration frequency, k is the force constant, and m is the effective mass. Similarly, the increasing pseudogaps for $Na_{0.3}CoO_2$ and $Na_{0.5}CoO_2$ mean a relatively strong covalent bonding between the parent atoms and thus an increasing phonon thermal conductivity.

The electrical conductivity for Na_xCoO_2 ($x = 0.3$, 0.5, 1.0) is presented in Fig. 3. With the decreasing Na content, the electrical conductivities at 1000 K increase from 21000 $\Omega^{-1}\cdot m^{-1}$ to 91000 $\Omega^{-1}\cdot m^{-1}$ and 141000 $\Omega^{-1}\cdot m^{-1}$, respectively, which are well consistent with the experimental data.[7] The difference in electrical conductivity is mainly resulted from the difference of their density of states, mobility of carriers as well as the band gap near the Fermi energy level.

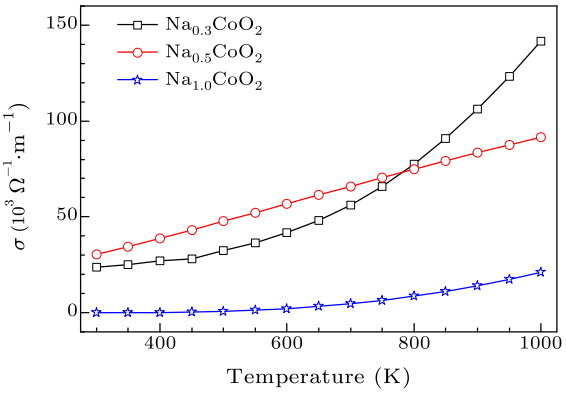

Fig. 3. Electrical conductivity of Na_xCoO_2.

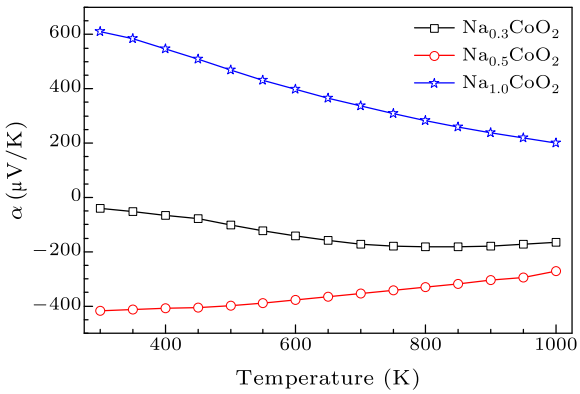

Fig. 4. Seebeck coefficient of Na_xCoO_2.

The Seebeck coefficient for Na_xCoO_2 ($x = 0.3$, 0.5, 1.0) is shown in Fig. 4. The negative sign of the Seebeck coefficients for $Na_{0.3}CoO_2$ and $Na_{0.5}CoO_2$ indicates that the major carriers are electrons over the whole temperature, while the main carriers in $Na_{1.0}CoO_2$ are holes. With the decreasing Na content, the Seebeck coefficients at 1000 K vary from $-165\,\mu V\cdot K^{-1}$ to $-271\,\mu V\cdot K^{-1}$ and $200\,\mu V\cdot K^{-1}$,

which are close to the experimental result.[26] Consequently, a maximum Seebeck coefficient can be obtained in $Na_{0.5}CoO_2$, which is ascribed to its broadened band gap, the increased effective mass of carriers and the small density of states near the Fermi energy level.

Figure 5 shows the power factor of Na_xCoO_2 (x = 0.3, 0.5, 1.0). It can be seen that with the decreasing Na content, the power factor of Na_xCoO_2 at 1000 K increases from 3.86 $mW{\cdot}m^{-1}{\cdot}K^{-2}$ to 6.73 $mW{\cdot}m^{-1}{\cdot}K^{-2}$ while then decreases to 0.85 $mW{\cdot}m^{-1}{\cdot}\ K^{-2}$. Thus an optimal power factor of 6.73 $mW{\cdot}m^{-1}{\cdot}K^{-2}$ is achieved in $Na_{0.5}CoO_2$ for its increasing electrical conductivity and the Seebeck coefficient.

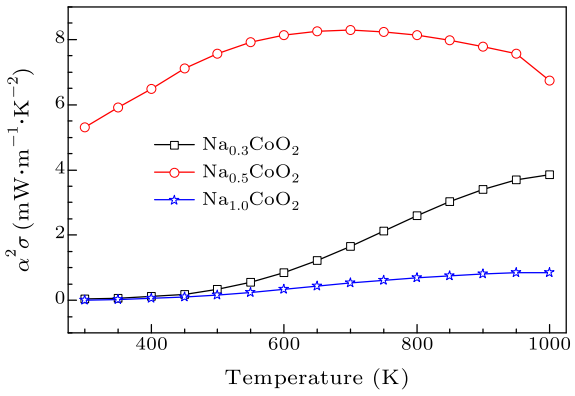

Fig. 5. The power factor of Na_xCoO_2.

In summary, the electronic structure and the power factor of Na_xCoO_2 (x = 0.3, 0.5, 1.0) have been calculated successfully using density functional theory and the Boltzmann transport theory. With the decreasing Na content, the DOS at the Fermi energy level increases and a transition from semiconductor to semimetal is observed, which consequently leads to an increasing electrical conductivity continuously. However, $Na_{0.5}CoO_2$ has an optimal Seebeck coefficient due to its broadened band gap near the Fermi energy level. Therefore, a maximum power factor is realized in $Na_{0.5}CoO_2$.

References

[1] Bell L E 2008 *Science* **321** 1457

[2] Snyder G J and Toberer E S 2008 *Nat. Mater.* **7** 105

[3] Takada K, Sakurai H, TakayamaMuromachi E, Izumi F, Dilanian R A and Sasaki T 2003 *Nature* **422** 53

[4] Ito M, Nagira T, Oda Y, Katsuyama S, Majima K and Nagai H 2002 *Mater. Trans.* **43** 601

[5] Seetawan T, Amornkitbamrung V, Burinprakhon T, Maensiri S, Tongbai P, Kurosaki K, Muta H, Uno M and Yamanaka S 2006 *J. Alloys Compd.* **416** 291

[6] Peleckis G, Motohashi T and Karppinen M 2003 *Appl. Phys. Lett.* **83** 5416

[7] Demchenko D O and Ameen D B 2014 *Comput. Mater. Sci.* **82** 219

[8] Tomoya N, Mikio I, Shigeru K, Kazuhiko M and Hiroshi N 2003 *J. Alloys Compd.* **348** 263

[9] Yakabe H, Fujita K, Nakamura K and Kikuchi K 1998 *Int. Conf. Thermoelectrics* (IEEE Service Center, Piscataway NJ United States, 24–28 May 1998) p 551

[10] Mrotzek A, Muller E, Plewa J and Altenburg H 2003 *International Conference On-ict* (IEEE Service Center, La Grande Motte France, 17–21 August 2003) p 219

[11] Tsai P H, Zhang T S, Donelson R, Tan T T and Li S 2011 *J. Alloys Compd.* **509** 5183

[12] Voneshen D J, Refson K, Borissenko E, Krisch E, Bosak M, Piovano A, Cemal A, Enderle E, Gutmann M J and Hoesch M 2013 *Nat. Mater.* **12** 1028

[13] Sun J and Guo Z P 2012 *Intergrated Ferroelectrics* **137** 120

[14] Yoshiya M, Okabayashi T, Tada M and Fisher C A J 2010 *J. Electron. Mater.* **39** 1681

[15] Jha P K, Troper A, Lima D C, Talatic I C and Sanyald S P 2005 *Physica* B **366** 153

[16] Tosawat S, Athorn V U, Prasarn C, Chanchana T and Vittaya A 2010 *Comput. Mater. Sci.* **49** S225

[17] Lynn J W, Huang Q, Brown C M, Miller V L, Foo M L, Schaak R E, Jones C Y, Mackey E A and Cava R J 2003 *Phys. Rev.* B **68** 214516

[18] Huang Q, Foo M L, Lynn J W, Zandbergen H W, Lawes G, Wang Y Y, Toby B H, Ramirez A P, Ong N P and Cava R J 2004 *J. Phys.: Condens. Matter* **16** 5803

[19] Takahashi Y, Gotoh Y and Akimoto J 2003 *J. Solid State Chem.* **172** 22

[20] Segall M D, Lindan P J D, Probert M J, Pickard C J, Hasnip P J, Clark S J and Payne M C 2002 *J. Phys.: Condens. Matter* **14** 2717

[21] Monkhorst H J and Pack J D 1976 *Phys. Rev.* B **13** 5188

[22] Stiewe C, Bertini L, Toprak M, Christensen M, Platzek D, Williams S, Gatti C, Müller E, Iversen B B, Muhammed M and Rowe M 2005 *J. Appl. Phys.* **97** 044317

[23] Kono Y, Ohya N, Taguchi T, Suekuni K, Takabatake T, Yamamoto S and Akai K 2010 *J. Appl. Phys.* **107** 123720

[24] Goldsmid H J and Sharp J W 1999 *J. Electron. Mater.* **28** 869

[25] Ziman J M 1972 *Principles of the Theory of Solid* (Cambridge: Cambridge University Press)

[26] Molenda J, Delmas C and Hagenmuller P 1983 *Solid State Ionics* **9** 431